

# NV Centres in Diamond

Corey Anderson

October 9, 2024

## 1 Introduction

Nitrogen-vacancy (NV) centers in diamond are point defects formed by a substituting a nitrogen atom adjacent to a vacant carbon site in the diamond lattice. These regions display quantum properties, including optical spin readout and long coherence times. The NV center's spin states, particularly the ground state spin triplet ( $|0\rangle$  and  $|\pm 1\rangle$ ), can be controlled and read out optically through photoluminescence, which changes depending on the spin state of the NV center. This investigation will cover techniques such as lock-in detection, optically detected magnetic resonance (ODMR), and spin coherence measurements to analyze the properties of NV centers.

## 2 Task 1

### 2.1 Lock-In Amplifier and PulseBlaster

This section involves setting up the equipment and checking lock-in amplifier receives the reference signal as expected. Lets model the method used by the lock-in amplifier to extract small signal. Let the input signal be:

$$V_i(t) = A \sin(\omega t + \phi) + N(t), \quad (1)$$

where the sinusoid is the desired signal and  $N(t)$  is the noise (1/f noise). The lock-in amplifier multiples  $V_i$  by the reference signal to get  $V_o$ , then puts  $V_o$  through a low pass filter. The reference signal is at the same frequency as the desired signal.

$$V_o = (A \sin(\omega t + \phi) + N(t)) \sin(\omega t) \quad (2)$$

$$= A \sin(\omega t + \phi) \sin(\omega t) + N(t) \sin(\omega t) \quad (3)$$

The noise can be represented by a sum of sinusoidal components at different frequencies. This gives the noise term as:

$$N(t) \sin(\omega t) = \sum_i B_i \sin(\omega_i t + \theta_i) \sin(\omega t) \quad (4)$$

$$= \frac{1}{2} \sum_i B_i [\cos((\omega_i - \omega)t + \theta_i) \quad (5)$$

$$- \cos((\omega_i + \omega)t + \theta_i)]. \quad (6)$$

Since noise is predominately 1/f noise, we have  $B_i \approx 0$  at sufficiently high frequencies, so those we can ignore. Considering the low frequency noise, that is,  $\omega_i \ll \omega$ ,

our two frequency components in the noise are

$$\begin{cases} \cos(\omega_i - \omega) \approx \cos(-\omega) = \cos(\omega) \\ \cos(\omega_i + \omega) \approx \cos(\omega) \end{cases} \quad (7)$$

After the LPF, the noise being approximately around the reference frequency  $\omega$ , is removed. Therefore, we have a high SNR.

Conversely, the signal part is:

$$A \sin(\omega t + \phi) \sin(\omega t) = \frac{A}{2} [\cos(\phi) - \cos(2\omega t + \phi)]. \quad (8)$$

After the LPF, the signal part reduces to  $\frac{A}{2} \cos(\phi)$  which is just a DC signal. Therefore, the resulting signal is

$$V_0 = \frac{A}{2} \cos(\phi) + (\text{negligible remaining noise}) \quad (9)$$

This is how a lock-in amplifier extracts the signal amongst relatively high noise environments.

### 2.2 Laser Modulation 1

**Q1. Explain why you get a non-zero DC value on the lock-in amplifier output?**

We have turned the green laser on and off at the same frequency as the reference signal (200 Hz) This modulates the photoluminescence from the NV sample at the same frequency. The lock-in amplifier measures the amplitude of the signal at the specific reference frequency of 200 Hz which means it outputs a DC value of 32 mV corresponding to the photoluminescence signal.

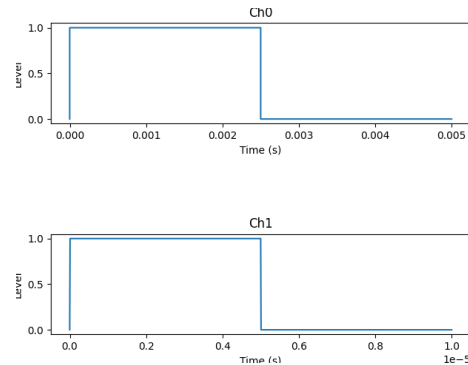


Figure 1: CH0: Reference, CH1: Laser

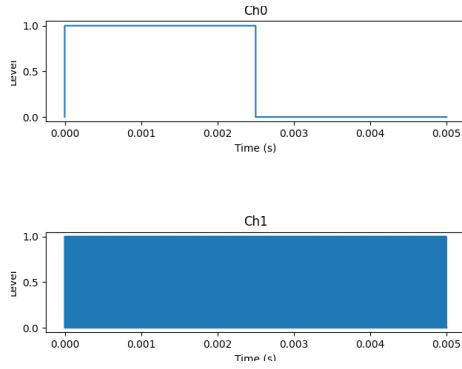


Figure 2: CH0: Reference, CH1: Laser

## 2.3 Laser Modulation 2

**Q2. Explain why the DC value goes to 0?**

We now change the pulse frequency to  $f_p = 100 \text{ kHz}$  while keeping the reference (CH0) frequency at  $f_r = 200 \text{ Hz}$ . We observed a 0 V output from the lock-in amplifier. This is because  $f_p \gg f_r$  so the high frequency pulses averages out over the much slower reference frequency. The photoluminescence signal now contains high frequency components at 100 kHz which arrives at the lock-in amplifier. However, since there are no frequency components around  $f_r$  anymore, the amplifier can not synchronise with any signal leading to a DC value of 0. This concept is equivalent to a significant number of phasors with different phases cancelling each other out.

## 2.4 Longitudinal Relaxation Time

In this section, we send in a initialisation pulse that polarises all the spins in the  $|0\rangle_g$  state. After a time delay of  $\tau$ , two readout pulses which have a  $180^\circ$  phase difference are sent in to measure the spin relaxation signal. Since the spin signals induced by the two pulses will be  $180^\circ$  out of phase, the lock-in amplifier can effectively differentiate and amplify this while ignoring the larger photoluminescence signal. To see this, let  $PL_0$  be the background photoluminescence signal and  $\Delta PL$  be the change in the signal due to the spin polarisation. The measured signal uses the two pulses detected by the amplifier:

$$\text{Signal} = P_1 - P_2 \quad (10)$$

$$= (PL_0 + \Delta PL) - (PL_0 - \Delta PL) \quad (11)$$

$$= 2\Delta PL \quad (12)$$

The signal is then normalised to the proper value which produces the relaxation curve Figure 3.

The reference frequency used is 21 Hz which is approximately 10 times less than the reference used in the first section. Which we see in the plot with the equilibrium voltage being 3.2 mV instead of 32 mV. The exponential fit gives us a relaxation time of  $T_1 = 0.76 \text{ ms}$ . This plot is actually the opposite of what we were expecting. The curve should decay which corresponds to transition from the  $|0\rangle_g$  state to the Boltzmann distributed

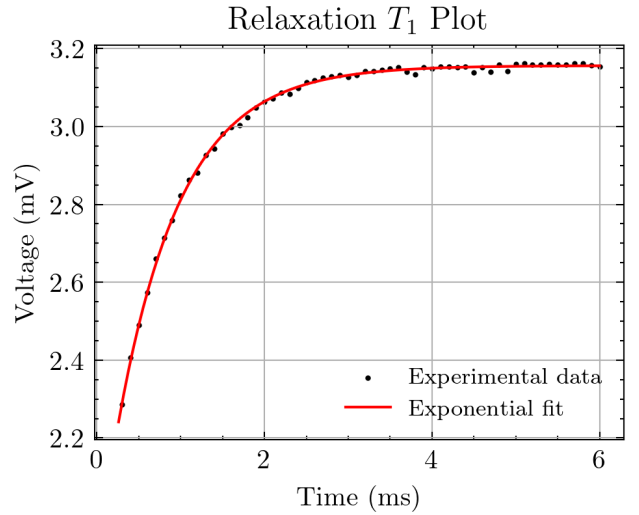


Figure 3:  $T_1$  Relaxation of spins initialised into the  $|0\rangle_g$  state

population. This is due to the  $|0\rangle_g$  state emitting more photons than the mixed state. The 3.16 mV offset is caused by the readout pulse being present in only one of the two half cycles of the reference signals. It therefore isn't filtered out completely by the lock-in amplifier.

## 2.5 Optically Detected Magnetic Resonance

**Q3. Explain why the microwave pulses must be modulated to follow the envelope of the reference signal?**

A microwave signal is now introduced to induce transitions between  $|0\rangle_g$  and  $|\pm 1\rangle_g$ . The microwave signals must have the same modulation frequency as the reference to focus on the microwave-induced effects on the photoluminescence signal due to the spin state transitions, while filtering out other uncorrelated noise and signals. The microwave and laser pulses are not overlapped because we want to control the transition between the ground spin states (microwave) and the optical excited spin transitions (laser pulses) independently, and not have these overshadow each other.

**Q4. At this point the lock-in amplifier output is still 0 V. Explain why this is the case?**

**Q5. What do you need to do to see a non-zero signal?**

The lock-in amplifier output is still 0 V because the frequency of the microwave pulses we are using is not the resonant frequency which will induce the ground state spin transitions. A microwave frequency satisfying  $hf_{mw} = \Delta E_{\text{spin}}$  will significantly increase the probability of spin transitions. Therefore, to see a non-zero signal, we need to be at the resonant frequency. To achieve this, a frequency sweep was carried out between 2.8 GHz and 2.95 GHz as shown in Figure 4:

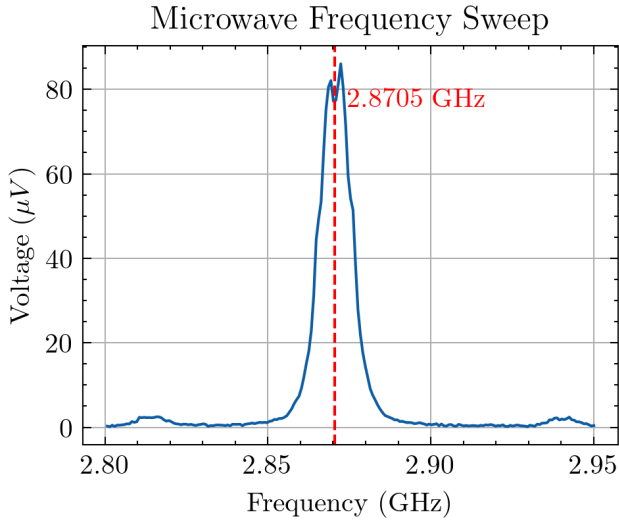


Figure 4: A microwave frequency sweep to plot the resonance of the ground spin state transitions

**Q6. Identify, describe and note down all the salient features you observe in your magnetic resonance sweep. Can you guess if there is an external magnetic field applied near your diamond sample?**

The resonance is at 2.8705 GHz which corresponds to a  $\Delta E = 11.87 \mu\text{eV}$ . Interestingly, we observe two small peaks. This suggests that there is a magnetic field which splits the degenerate  $|\pm 1\rangle_g$  states. The magnetic field is induced by defects in the material which inhibits the magnetic domains from completely cancelling out.

## 3 Task 2

### 3.1 Optically Detected Magnetic Resonance

The  $|\pm 1\rangle$  states are degenerate under 0 magnetic field. We now apply a magnetic field which is produced current passing through coils. This causes Zeeman splitting of the  $|\pm 1\rangle$  states.

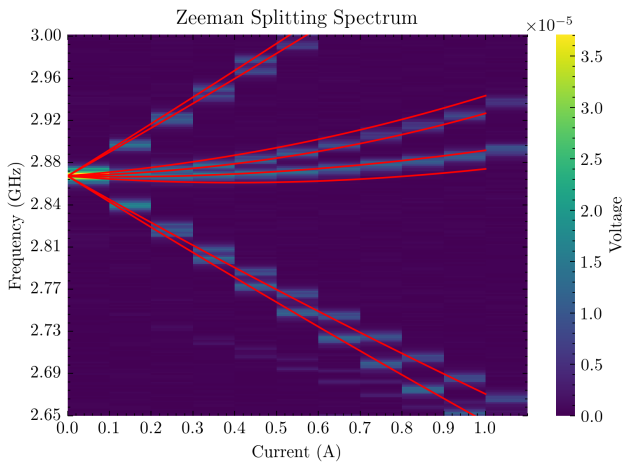


Figure 5: Heat map of Zeeman splitting of Resonance peaks

**Q3. Carefully note the various salient features of the ODMR spectra. How many resonance peaks can be observed? How many do we expect to see? Do all the resonance peaks react to a change in coil current amplitude in the same way?**

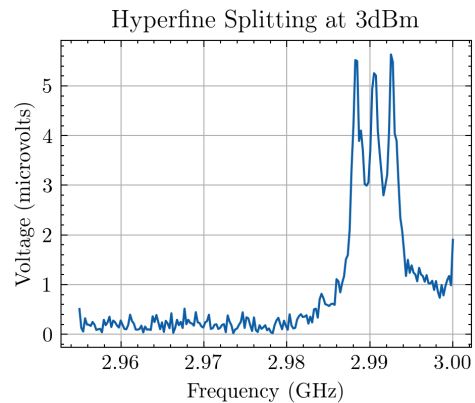
The NV center has 4 possible orientations and we have 2 possible state transitions under microwave excitation;  $|0\rangle$  to  $|1\rangle$ , and  $|0\rangle$  to  $|-1\rangle$ . Therefore we expect 8 peaks in the spectrum when a magnetic field is applied to the diamond sample. As seen in fig. 5 we only see 6 peaks in the spectrum which suggests that the missing peak is due to 2 of the orientations being very similar, hence our inability to resolve them. We also see a faint peak which is a result of hyperfine splitting of the NV spins that are also coupled to a  $C^{13}$  nucleus. The energy splitting of the states depends on the orientation of the magnetic field with respect to the NV axis, which allow us to distinguish between the 4 different orientations using our spectra.

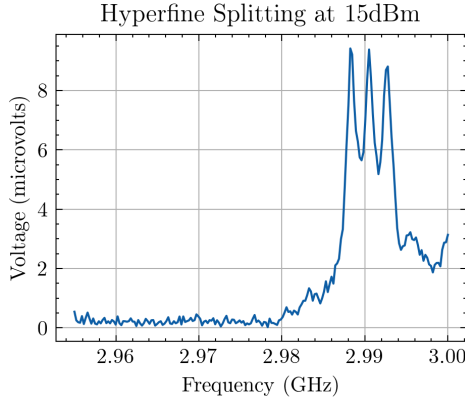
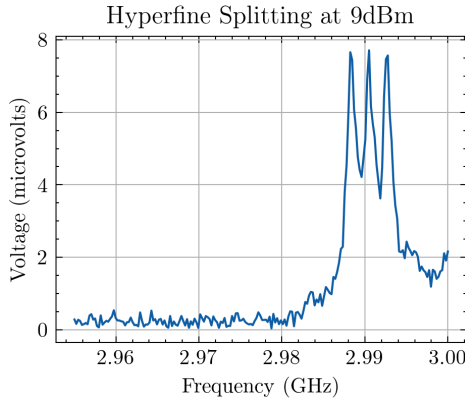
We have also simulated the NV centre's Hamiltonian in order to find out the orientation of the magnetic field with respect to the sample. We found agreement between theory and experiment using coil constant of  $0.02 \text{ T A}^{-1}$  and an orientation vector of  $(0.5, 0.6, 0.05)$

### 3.2 The Hyperfine Splitting

In the negatively charged NV center, the defect has an unpaired electron whose spin interacts with the spin of the  $^{14}\text{N}$  nucleus. This interaction causes a small energy splitting of the nuclear spin states ( $m = -1, 0, +1$ ) which observable in the low-field regime.

For this experiment, we set the external magnetic field to 0.005 T using the coil with the previously determined coil constant. An ODMR experiment was then conducted at various microwave powers (15 dBm, 9 dBm, and 3 dBm) to investigate the effect of microwave power on the resonance peaks.





**Q4.** Observe and note down all the salient features of the ODMR spectra. How many peaks do you observe? How far apart are the peaks from each other? Would you expect these peaks to move further apart when the magnetic field is increased? Can you guess the spin quantum number of the  $^{14}\text{N}$  nuclei that the vacancy is coupled to based on the number of peaks you can observe?

**Q5.** What effect did reducing the microwave power have on the ODMR spectra?

We observe a very slight reduction in the width of the peaks when the microwave power is reduced. However our peak barely narrowed which suggests an error with the apparatus or code setup. We observe 3 peaks corresponding to the 3 nuclear spin states. The separation between the peaks corresponds to the strength of the hyperfine interaction and we found it to be around 2.9 MHz. The fact that we get 3 peaks indicates that the nuclear spin of the NV center is interacting with a spin-1 system. This is due to 2 unpaired electrons localized at the NV defect site. If the magnetic field is increased, we would expect the hyperfine peaks to move further apart due to the Zeeman interaction splitting the states further apart.

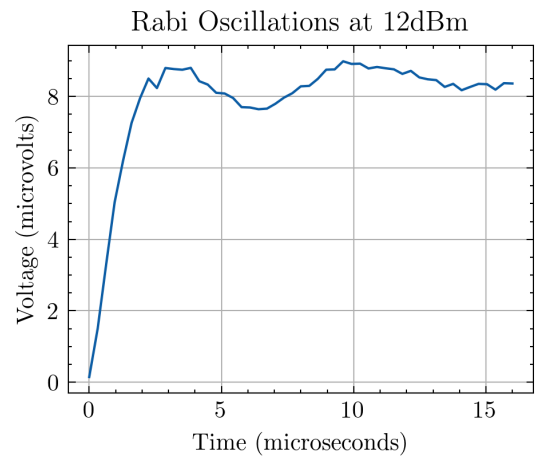
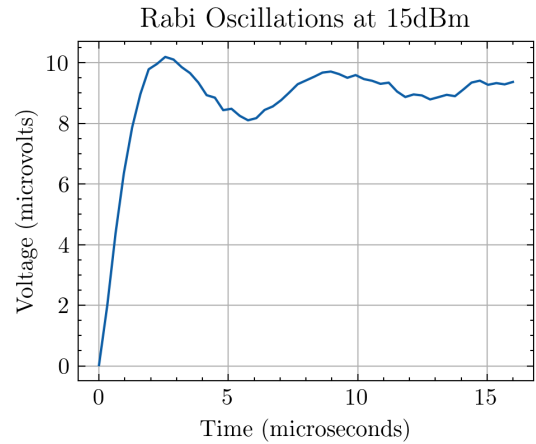
### 3.3 Rabi Oscillations

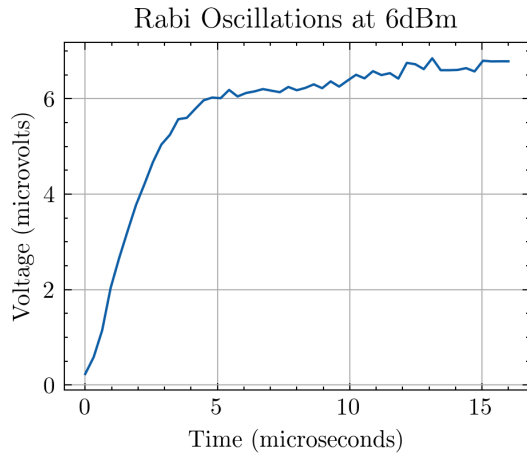
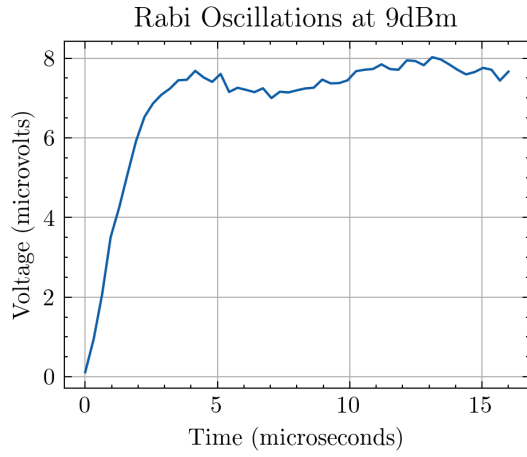
We now investigate the behavior of Rabi oscillations in the NV center's spin system by applying microwave pulses at a chosen resonance frequency obtained from the ODMR spectra. We begin by selecting the res-

onance peak with the lowest frequency, identified at 2.99262 GHz, and setting the microwave source to this frequency. The NV centre's spin state undergoes coherent rotation between the  $|0\rangle$  and  $|\pm 1\rangle$  states with a frequency known as the Rabi frequency, which is detected as oscillations in the photoluminescence intensity by our instruments.

**Q5.** Do you observe any relationship between the microwave power and the oscillation frequency of the signal? By how much must the microwave source be attenuated for the Rabi frequency to be changed by a factor of 2? Furthermore, are the oscillations completely sinusoidal at lower powers? Explain why this could be the case

We change the power of the microwave pulses while monitoring the changes in the PL intensity, this changes the angle by which the spin rotates during the application of the microwave field, affecting the probability of transition between spin states. More powerful pulses result in larger rotational angles, leading to the observation of full Rabi oscillations. This is seen in the plots with the highest power microwave pulses resulting in larger oscillations:





The Rabi frequency is proportional to the the magnetic field amplitude

$$\omega_1 \propto B_1 \propto \sqrt{P} \Rightarrow P \propto \omega_1^2 \quad (13)$$

Thus, to increase the Rabi frequency by 2, we must increase the applied power by 4 (+6 dBm) which is approximately what we see in the 9 dBm and 15 dBm plots. At lower powers, the oscillation tends to be less sinusoidal due to increased decoherence and insufficient driving strength to induce coherent rotations. This is summarised by the Rabi formula:

$$P_{-1} = |\langle -1 | \psi(t) \rangle|^2 \quad (14)$$

$$= \frac{(\frac{1}{2}\omega_1)^2}{\Delta\omega^2 + (\frac{1}{2}\omega_1)^2} \sin^2 \left( \frac{1}{2} \sqrt{\Delta\omega^2 + \left(\frac{1}{2}\omega_1\right)^2} t \right) \quad (15)$$

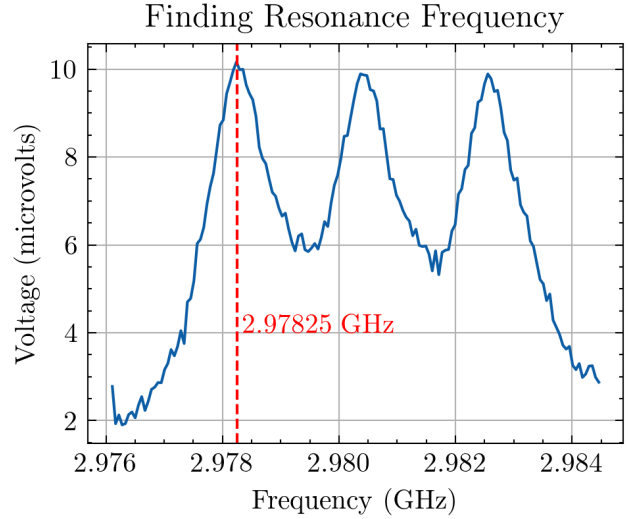
This is in the form of a Lorentz curve with FWHM of  $\frac{1}{2}\omega_1$ . Thus, when the microwave power is increased, the FWHM of the curve increases so individual oscillations are harder to resolve.

## 4 Task 3

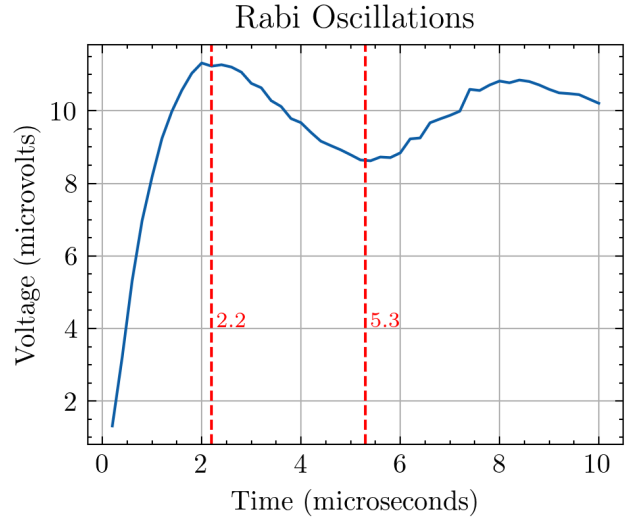
### 4.1 Ramsey Fringes

Ramsey fringes are a technique used to determine the coherence properties of the NV center. It consists of

two  $\pi/2$  pulses separated by a free precession time. The first pulse creates a superposition state, causing the spins to precess in the xy-plane of the Bloch sphere, accumulating a phase and reducing the polarisation. The second pulse converts this accumulated phase a population difference, which can be read out optically. We first need to find the time  $T_{X\pi}$  needed to rotate the spins from  $|0\rangle$  to  $|+1\rangle$  about the x-axis of the Bloch sphere. To do so we will measure the Rabi frequency using ODMR where the frequencies are swept and the lowest peak is observed as shown in section 4.1 Set-

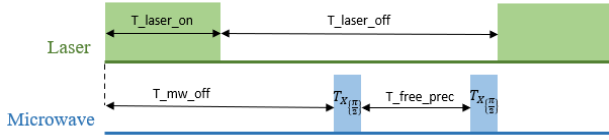


ting the microwave frequency to the lowest transition resonant frequency, we obtain the following Rabi oscillations

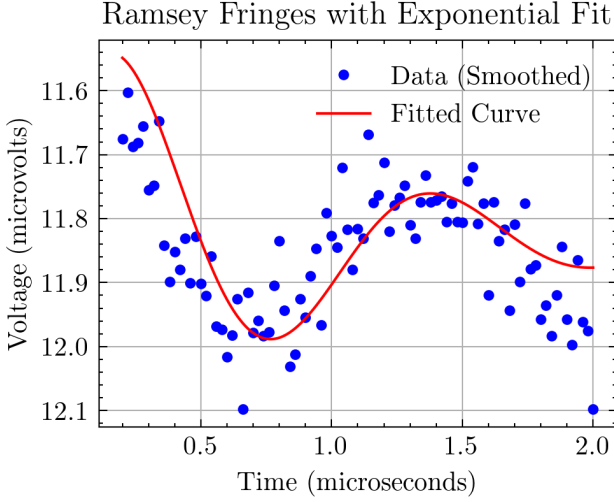


where the time difference between the extremities of the graph corresponds to  $T_{X\pi} = 3.1 \mu s$ . Now that these parameters are obtained, we can measure the dephasing time  $T_2^*$  which is done by measuring the decay time of the Ramsey fringes by applying the following gates:  $R_x(\pi/2) \rightarrow \tau \rightarrow R_x(\pi/2)$ . I.e. the pulse sequence is given by

Due to some unknown reason, the Ramsey curve decayed upwards which might be a systematic error re-



lating to the apparatus used. I have flipped the plot vertically to solve this issue.



The fitting of an exponentially decaying sinusoid gives  $T_2^* = 0.905 \mu\text{s}$  which is a measure of the decoherence time in the Ramsey experiment. The presence of oscillations tell us that we are not exactly on resonance and the loss of polarisation is observed in the decaying of the oscillations. The accuracy and fitting of the  $T_2^*$  time would have benefited from a longer time to obtain more oscillations.

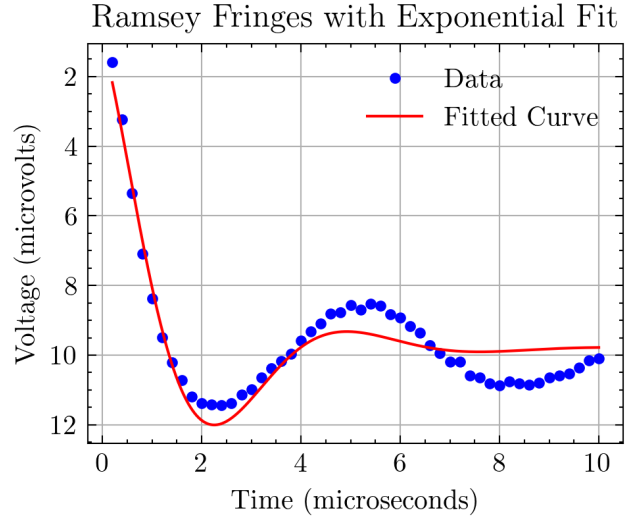
**Q1. Comment on the feature of your Ramsey experiment. In particular, comment on the direction of the decay, and the frequency of the oscillations.**

As mentioned, the decay is initially up which is the opposite to what we expect. A downward decay is expected because the net result of the 2  $R_x(\pi/2)$  rotations is transitions from  $|0\rangle$  to  $|+1\rangle$ . The fitted frequency is 819 kHz which indicates a detuning of the applied pulses. The detuning is not that substantial given the resonance frequency was 2.98 GHz.

## 4.2 Two Axes Controlled Ramsey decay

This time, another input using Channel 3 is implemented such that the IQ modulation is carried out. This allows us to perform rotations in both the X and Y axis. We will now repeat the Ramsey experiment with an XY pulse sequence. The first microwave pulse produces a  $R_x(\pi/2)$  rotation and the second pulse produces a  $R_y(\pi/2)$  rotation. The goal of the second pulse is to remove the noise present in the system.

This time we get  $T_2^* = 1.75 \mu\text{s}$  which is much longer



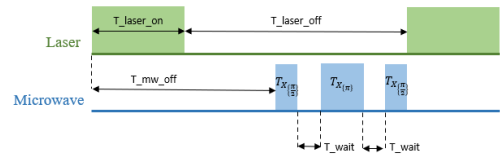
than our initial Ramsey experiment, demonstrating that the  $R_y(\pi/2)$  successfully removed some of the noise present in the system, and thus increasing the coherence time. For some reason, the fitting isn't very accurate which may lead to some errors in the  $T_2^*$  time given.

## 4.3 The Hahn Echo

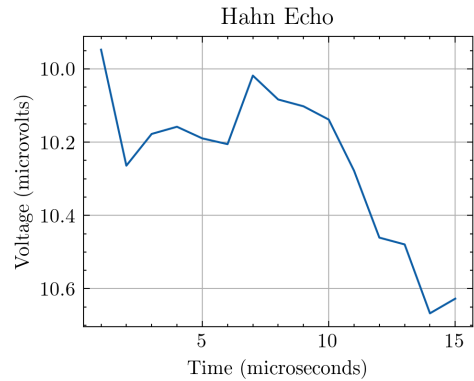
*Credit to Antony Radman for the Hahn Echo and the CPMG data.*

The Hahn Echo sequence introduces an additional pulse:

$$R_X\left(\frac{\pi}{2}\right) \rightarrow \tau \rightarrow R_X(\pi) \rightarrow \tau \rightarrow R_X\left(\frac{\pi}{2}\right) \quad (16)$$



This pulse sequence generated the results as shown below:



Again, the data was flipped to what we expect so I inverted the the graph. I was not able to perform a



fit due to the bad data but the  $T_2^H$  time does seem to be much longer than the Ramsey. The spins first get initialised into the  $|-z\rangle$  state and the first  $\pi/2$  pulse rotates it to the  $|+y\rangle$  axis where it precesses around the xy-plane due to noise decoherence. The  $\pi$  pulse then rotates it to the  $|-y\rangle$  state where the spins are refocused. The second  $\pi/2$  brings the spins back to the  $|-z\rangle$  state. This refocusing of spins therefore remove the DC noise that was present during the Ramsey

**Q2. Record your  $T_2^H$  time. Do you expect this to be longer or shorter than  $T_2^*$ ? Secondly, explain why you expect the signal to decay in the direction that it does.**

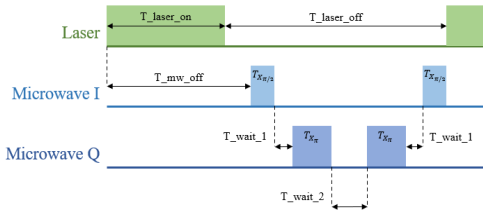
$T_2$  time is not calculated because the data is not appropriate for a fit. I expect this to be longer than Ramsey due to the removal of DC noise. The graph starts high since all spins are in the bright ground  $|0\rangle$ . After rotation, we get dephasing leading to the decay in the plot. The plot peaks again due to the refocusing pulse.

#### 4.4 CPMG

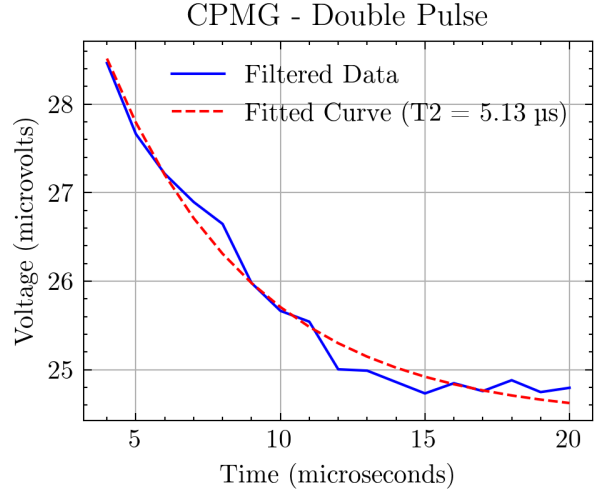
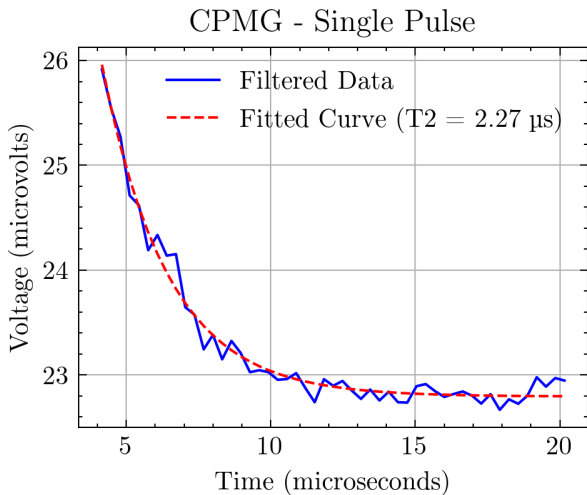
The CPMG is an improvement to the Hahn Echo by sampling lower amounts of noise in the higher frequencies. The 2-pulse sequence looks like

$$R_x(\pi/2) \rightarrow R_y(\pi) \rightarrow R_y(\pi) \rightarrow R_x(\pi/2) \quad (17)$$

and the 1-pulse CPMG is the same but removing a  $R_y(\pi)$  pulse. The sequence is implemented using the following pulses:



Doing so gives the following results for the single and double pulse sequences:



Fitting an exponential to both plots give the times of  $T_2^{CPMG1} = 2.27 \mu s$  and  $T_2^{CPMG2} = 5.13 \mu s$ .

**Q3. For a particular  $\tau$ , how do the center frequencies of the bandpass filter functions created by the 3 different CPMG pulse sequences compare? Based on this understanding, what type of noise is most likely associated with the dephasing of the spins? Finally, as before, explain why a CPMG pulse sequence decays in the direction that you observe in your experiment?**

The reason for a higher  $T_2$  time for the 2-pulse is due to the noise being sampled at higher frequencies where the magnitude of noise is a lot less. Therefore, the noise is characterised by low frequency noise so likely  $1/f$  noise. The decay is due to the interaction of the spins with the environment, leading to a loss of coherence over time. The decay is slower for the double pulse for reasons mentioned previously.

## 5 Conclusion

Through a series of experiments involving lock-in detection, microwave modulation, and Ramsey and Hahn Echo sequences, the properties of NV centers in diamond were thoroughly analyzed. The  $T_1$  and  $T_2^*$  relaxation times were measured for the different sequences, which helped me understand the spin dynamics and coherence of the NV centers. The ODMR spectra revealed the effects of external magnetic fields, including Zeeman splitting and hyperfine interactions. Additionally, Rabi oscillations and the application of multi-pulse sequences such as Hahn Echo and CPMG demonstrated the role of environmental noise in the decoherence of the spin states.